International Journal of Environmental Sciences
ISSN: 2229-7359
Vol. 11 No. 21s, 2025
https://theaspd.com/index.php

Programmable and Flexible Stimulator for Neuromuscular FES

M.A.M.A Halim[1], E. Noorsal[1*], K. Sooksood[2], S.Z. Yahaya[3], Z. Hussain[1], S.Z.M. Saad[1], M.H. Abdullah[1], S. Setumin[1]

[1]Electrical Engineering Studies, Universiti Teknologi MARA, Cawangan Pulau Pinang, Permatang Pauh, 13500, Pulau Pinang, Malaysia.

[2]Department of Electronics Engineering, School of Engineering, King Mongkut's Institute of Technology Ladkrabang, Bangkok 10520, Thailand.

Corresponding Author: *emilia.noorsal@uitm.edu.my

ABSTRACT:

This paper presents the design of a programmable and flexible stimulator that generates biphasic stimulation waveforms for neuromuscular Functional Electrical Stimulation (FES). The FES device facilitates muscle contraction in the paralyzed limbs of spinal cord injury (SCI) patients by delivering low electrical pulses through electrode pads. A major challenge in FES-induced muscle contraction is early muscle fatigue, which significantly limits activities such as FES-assisted standing and walking. The use of a fixed stimulation pattern, typically a rectangular waveform, repeatedly activates the same motor units, leading to overwork and rapid fatigue. To address this limitation, this work proposes a programmable and flexible stimulator using an Arduino Mega 2560 microcontroller and biphasic output current source circuits. The stimulator allows for adjustable stimulus parameters, including biphasic output current (0–100 mA), pulse width (2 µs–20 ms), and frequency (20 Hz–2 kHz). Additionally, the system supports multiple waveform shapes, including rectangular, ramp-up/down, triangular, trapezoidal, exponential up/down, and burst pulses. The biphasic output current circuit was chosen for its safety advantages, as it prevents residual charge accumulation on the electrodes, reducing the risk of skin burns. The proposed design was first simulated using Proteus 8 software before being implemented and tested on hardware. The simulation and hardware measurement results confirmed and validated the stimulator's functionality, demonstrating its ability to meet the specified design requirements.

KEYWORDS: *Functional Electrical Stimulation (FES), Spinal Cord Injury (SCI), Programmable and flexible stimulation waveform, Biphasic Output Current Source, Arduino Microcontroller, Graphical User Interface, Neuromuscular.*

1 INTRODUCTION

Functional electrical stimulation (FES) is a well-established rehabilitation method that applies electrical impulses to elicit muscle contractions, thereby supporting muscle re-education and helping to prevent atrophy in individuals affected by spinal cord injuries or neurological disorders [1], [2], [3]. By triggering controlled contractions of paralyzed or weakened muscles, FES devices maintain muscle activity and mitigate atrophy in patients with limited mobility [4], [5], enhancing muscle control and strength through targeted stimulation [6]. However, rapid muscle fatigue remains a persistent challenge in FES rehabilitation [7].

Conventional FES systems typically rely on fixed, rectangular pulse waveforms with limited parameter flexibility [8]. Such non-flexible stimulation can precipitate early fatigue because it continuously generates simultaneous action potentials in motor neurons [9], [10], leading to quicker fatigue onset and reduced muscle performance [7], [11]. Moreover, the inability to customize pulse shapes and stimulation parameters constrains the potential to optimize FES protocols for individual patient requirements [12], [13], [14]. Recognizing these limitations, several studies have advocated for alternative waveform shapes—such as trapezoidal, triangular, and exponential—that may help delay fatigue by modulating how motor units are activated [8], [15], [16], [17].

Recent research on non-rectangular stimulation underscores the benefits of flexible waveforms. For example, quasi trapezoidal and triangular pulses have been shown to achieve selective stimulation of certain nerve fibres while reducing activation of unwanted fibres [18], [19]. Exponential pulse shapes can diminish power consumption, lower charge injection, and mitigate safety risks [12], [20]. Additionally, Gaussian or sinusoidal stimuli produce substantially smaller peak current densities when compared to square pulses,

thereby enhancing safety [21]. These findings highlight that flexible waveform generation is pivotal for improving FES outcomes and potentially minimizing the impact of early muscle fatigue.

Despite growing recognition of the advantages associated with non-rectangular pulses, many FES devices still employ rigid waveforms and predefined stimulation parameters [7], [22]. A flexible, programmable FES system that allows the clinician or user to configure wave shape, frequency, amplitude, and pulse width would facilitate patient-specific optimization and may lead to better rehabilitation results [9], [10]. Advances in microcontroller-based designs have made it increasingly feasible to integrate multiple stimulation patterns into a single device [23]. Such flexibility enables broader applicability in rehabilitation contexts and can provide a platform for testing diverse stimulation strategies aimed at mitigating fatigue and maximizing muscle performance.

This paper presents the design and development of a programmable flexible biphasic waveform stimulator tailored for FES applications and accompanied by a graphical user interface (GUI) to facilitate user interaction. The system can generate multiple biphasic waveforms—Ramp Up, Ramp Down, Triangle, Trapezoidal, Burst Pulse, and Exponential—with adjustable parameters that include current amplitude peak-to-peak of 0–100 mA, pulse width 2–20000 μs, and frequency of 20–2000 Hz. The key objectives of this work are to design and implement this versatile waveform stimulator, achieve precise timing control using an Arduino microcontroller, and validate the system's functionality and output accuracy through Proteus simulation and hardware measurements. By offering customized and verifiable stimulation patterns, the proposed solution addresses current limitations in conventional FES devices and provides a practical platform to explore fatigue-mitigation strategies.

2 LITERATURE REVIEW

This section examines key advances and persistent challenges in functional electrical stimulation (FES), particularly regarding waveform design. It highlights the fundamental role of FES in rehabilitation, explores how rigid stimulation parameters can exacerbate muscle fatigue, and emphasizes the benefits of flexible and programmable biphasic waveforms for more effective muscle activation.

2.1 Functional Electrical Stimulation (FES)

FES is frequently employed to rehabilitate muscles in individuals with spinal cord injuries (SCI) or neurological disorders [2], [3]. By delivering electrical impulses that elicit muscle contractions, FES devices help maintain muscle mass, counteract atrophy, and potentially mitigate fatigue in people with limited mobility [4], [5]. Moreover, FES can facilitate re-education of impaired nerves, enabling more efficient muscle control for activities such as gait training, load distribution during ambulation, and even specific tasks like relearning swallowing mechanisms in post-stroke conditions [6].

High-frequency stimulation is sometimes used to produce smoother muscle contractions, but it can also hasten the onset of fatigue [9], [10]. Thus, many existing single-pattern FES devices fail to account for physiological recruitment dynamics. The result is diminished torque output and shortened rehabilitation duration—both of which pose significant barriers to comprehensive rehabilitation.

2.2 Disadvantages of Fixed, Non-Programmable Waveforms

Many FES systems rely on fixed stimulation waveforms, offering limited or no programmability in parameters such as pulse width, frequency, or amplitude [24]. This rigidity hinders customization for individual patient needs, often leading to suboptimal rehabilitative outcomes. Without the ability to adjust stimulation settings dynamically, it becomes difficult to counteract rapid fatigue, as the same motor units are repeatedly stimulated without sufficient rest [9].

Because these systems cannot tailor stimulation to patient-specific muscle characteristics, they often fail to mimic the natural variability in muscle recruitment. Consequently, the duration of effective rehabilitation is curtailed, and long-term rehabilitation gains are compromised [9]. These limitations underscore the pressing need for more sophisticated FES devices capable of offering adjustable waveforms and stimulation parameters.

2.3 Flexible and Programmable Biphasic Stimulation Waveforms and Advantages

Flexible and programmable FES approaches allow real-time modification of stimulus parameters—such as amplitude, frequency, and pulse shape—to better tailor electrical stimulation to individual patient needs.

For instance, Noorsal et al. [9] demonstrated that non-rectangular waveforms, including triangular, ramp-up, and ramp-down pulses, can significantly delay early muscle fatigue compared to conventional rectangular or trapezoidal pulses. Mercado-Gutierrez et al. [14] further showed the benefits of a pulse stimulator capable of co-modulating frequency and pulse width to improve muscle activation during functional tasks. Additional work by Nath et al. [13] revealed that delivering biphasic pulses with user-defined parameters reduces potentially harmful residual charges, while other studies have shown that flexible biphasic waveforms enhance comfort and energy efficiency and minimize tissue damage [12]. Collectively, these findings suggest that programmable waveform strategies optimize muscle performance, mitigate premature fatigue, and accommodate the distinct physiological profiles of individual patients [25].

Moreover, enabling clinicians or end-users to configure specific waveform parameters—such as shape, pulse duration, and current amplitude—can substantially improve FES interventions. By adjusting stimulation to match each patient's muscle properties, flexible systems can slow the onset of fatigue, increase functional torque output, and extend the period of effective stimulation [22], [26]. Tailored biphasic waveforms also align more closely with natural muscle recruitment patterns, reducing the strain on any single group of motor units and helping to maintain muscle force over longer periods. Overall, dynamic waveform customization through flexible, programmable devices is better positioned to address patient variability and enhance rehabilitation outcomes. These advantages have motivated the development of the present flexible biphasic waveform stimulator, which features a user-friendly interface for rapid, clinically driven adjustments of key stimulation parameters.

3 SYSTEM ARCHITECTURE

This research aims to design a programmable and flexible FES capable of adjusting stimulus parameters within predefined ranges and generating various stimulation shapes, as detailed in Table 2.

3.1 System Overview

Figure 1 illustrates the overall system of the proposed programmable and flexible protocol, which comprises a GUI, a microcontroller (Arduino Mega 2560), an analogue circuit, and electrode. FES waveform generation consists of three main components: a microcontroller for digital waveform generation, a digital-to-analog converter (DAC) circuit, and a biphasic analog output stage.

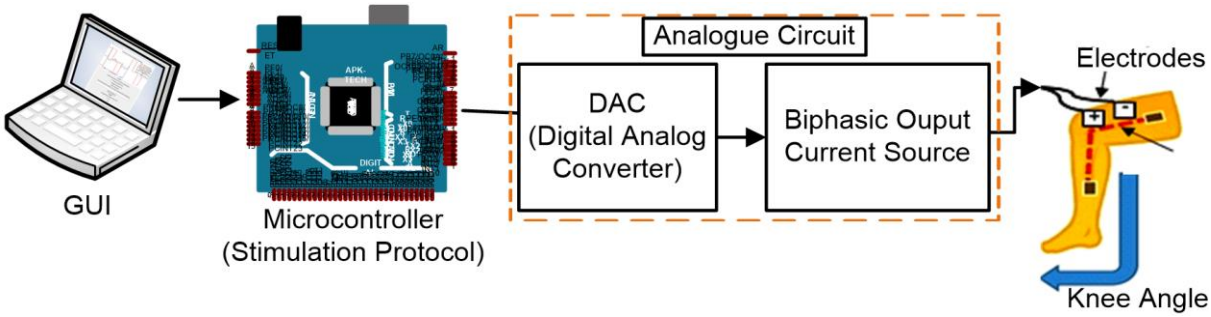

Figure 1: System Overview.

As previously mentioned, the FES-assisted device is used in the rehabilitation of spinal cord injury (SCI) patients to help restore motor functions in paralysed muscles by delivering a stimulus charge to the affected areas. Users configure stimulus parameters through the GUI, based on the user's preference onto the microcontroller to generate the desired stimulation waveform. The DAC circuit converts programmed parameters into analogue signals, which are then amplified and delivered to the load through the biphasic output current source circuit.

3.2 Digital-to-Analog Conversion

As shown in Figure 2, the DAC stage employs a DAC0800 high-speed monolithic converter that processes 8-bit input from the Arduino Mega 2560. The DAC circuit incorporates voltage reference components and filtering capacitors to ensure stable conversion. The circuit can generate output currents up to 20mA, with the converted analog signal being directed to the biphasic output stage for further amplification. In this way, the analogue output is converted into the desired biphasic waveform and ultimately delivered to the stimulation electrode.

International Journal of Environmental Sciences
ISSN: 2229-7359
Vol. 11 No. 21s, 2025
https://theaspd.com/index.php

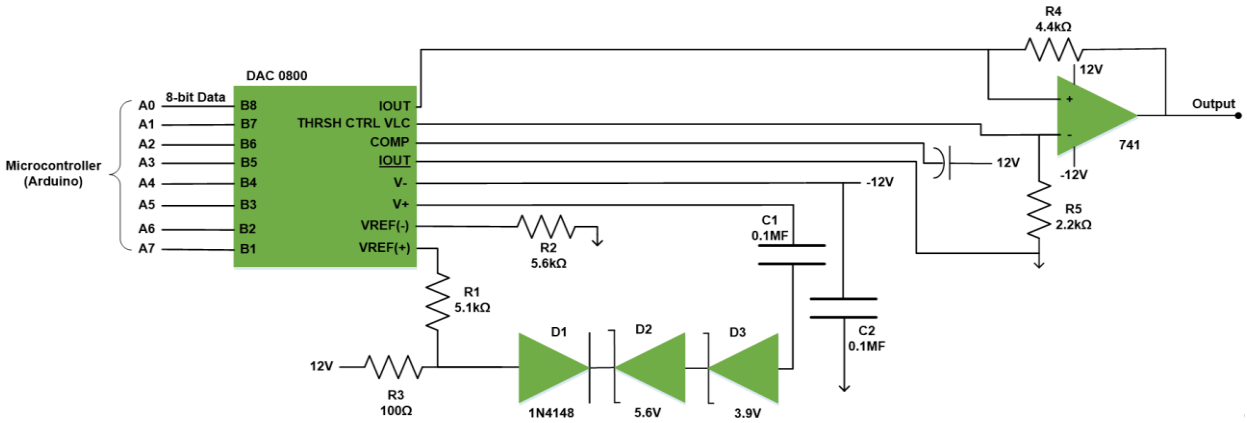

Figure 2: DAC Circuit.

3.3 Biphasic Output Circuit

The biphasic output stage, depicted in Figure 3, comprises four key components: non-inverting amplifier, inverting amplifier, summing amplifier, and an improved Howland charge pump. This configuration enables the generation of both positive and negative phases of the stimulation waveform ensuring charge balance to minimize tissue damage. The circuit employs three LM741 operational amplifiers for signal conditioning and an OPA454 high-current operational amplifier in the Howland charge pump configuration. Two 74HC4016 switches (SW1 and SW2) control the timing between positive and negative phases, with the microcontroller managing the switching sequence.

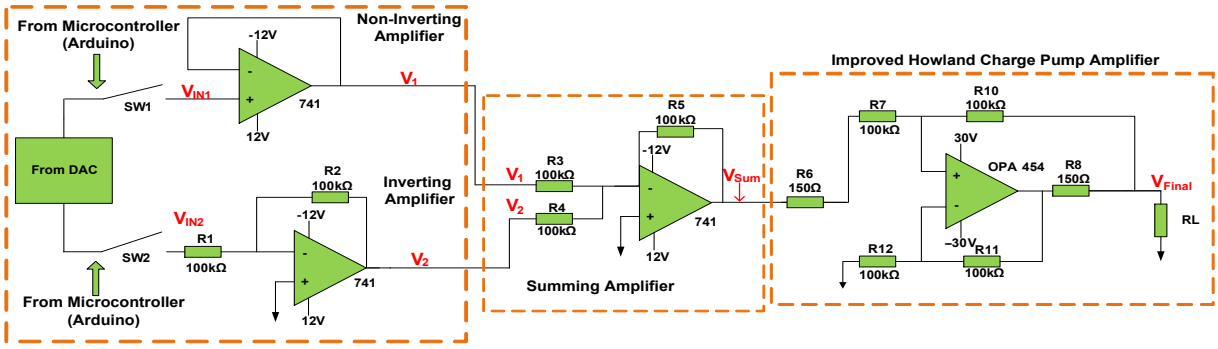

Figure 3: Biphasic Output Circuit.

1. Non-Inverting Amplifier

This stage is built around an LM741 operational amplifier powered by ±12 V. It receives a 5 V pulse from the microcontroller (Arduino) through the 74HC4016 switch (SW1). The amplifier's gain is set via (1):

$$\frac{\text{Vout}}{\text{Vin}} = 1 + \frac{\text{Rf}}{\text{Rin}} \tag{1}$$

In this design, there is no additional feedback resistor, so the gain effectively equals 1, preserving the original pulse polarity as a positive-going signal $V_{NON\text{-}INV}$.

2. Inverting Amplifier

A second LM741 powered by ±12 V produces a negative polarity signal, offset by 800 µs (example user input value) via the 74HC4016 switch (SW2). This timing offset ensures that the inverting pulse does not overlap with the non-inverting pulse. Its gain is determined by (2):

$$\frac{\text{Vout}}{\text{Vin}} = -\frac{\text{Rf}}{\text{Rin}} \tag{2}$$

With both R_f and R_{in} chosen as 100 kΩ, the gain is −1, flipping the pulse to a negative waveform V_{INV}.

3. Summing Amplifier

The summing amplifier (another LM741 at ±12 V) combines $V_{NON-INV}$ and V_{INV} into a unified biphasic output V_{sum}. Its output is governed by (3):

$$\text{Vout} = -\frac{\text{Rf}}{\text{Rin}}\,[\text{V1} + \text{V2} + \cdots] \tag{3}$$

where V_1=$V_{NON-INV}$ and V_2=V_{INV}. The resulting biphasic signal has a peak-to-peak voltage equal to the sum of the inverting and non-inverting amplitudes.

4. Improved Howland Charge Pump

The final stage is implemented with an OPA454 high-current operational amplifier at ±50 V_{pp}. By configuring the amplifier in an Improved Howland topology, the output is converted from a voltage signal V_{sum} into a stable current I_{Final}. This design allows up to 100 mA peak-to-peak of output current, addressing the higher current demands often required in FES. The OPA454's wide supply range ensures adequate headroom to drive larger load resistances without performance degradation.

Figure 3 details each op-amp stage and its respective functions, switching elements, and resistor networks. Equations (1)–(3) govern the gain and polarity transformations that produce a biphasic stimulation pulse. By carefully selecting component values (see Table 1), the circuit can be configured to produce waveforms with customizable amplitude, polarity timing, and current output vital properties for efficient functional electrical stimulation.

Table 1. List of components used in programmable biphasic circuit.

Components	Values
LM 741	-
OPA 454	-
Switch (74HC4016)	-
Resistor (at switch for non-inverting, R18)	3kΩ
Resistor (R1, R2, R3, R4, R5, R7, R9, R10, R11, R12)	100kΩ
Resistor (R6 and R8)	150Ω
Resistor (RL)	500Ω/1kΩ/2kΩ

4 METHODOLOGY

Figure 4 outlines the step-by-step methodology for developing a flexible and programmable biphasic output for FES. The process begins by defining the project specifications, including the required output current range and stability parameters, which establish the foundation for subsequent design steps. Next, the biphasic output current circuit is created in the Proteus simulation environment, focusing on component selection and arrangement to achieve the desired output characteristics. At the core of the system, flexible code is developed in the Arduino Integrated Development Environment (IDE) to control generation of the biphasic output according to the defined specifications. Once coded, the Arduino program is compiled and simulated within Proteus, enabling a thorough evaluation and verification of the biphasic waveform prior to hardware implementation. This final validation step confirms that the system meets the initial objectives for FES applications.

This methodology provides a systematic framework, encompassing design specifications, circuit implementation, and simulation-based validation for producing reliable FES waveforms. As shown in Figure 4, the integrated process supports a robust, programmable and flexible solution capable of delivering various biphasic stimulation patterns for rehabilitation purposes.

International Journal of Environmental Sciences
ISSN: 2229-7359
Vol. 11 No. 21s, 2025
https://theaspd.com/index.php

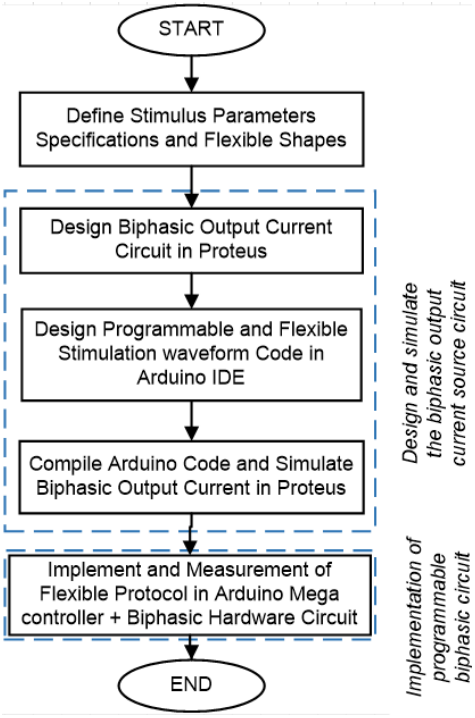

Figure 4: Overall research methodology.

4.1 Design Specification for Programmable and Flexible Stimulator

Table 2 summarises the key specifications and waveform types for the proposed programmable and flexible stimulator, intended for controlled electrical muscle stimulation in rehabilitative settings. The Amplitude (V_{pp}) parameter (0–50 V_{pp}) defines the peak-to-peak voltage level of the pulse, directly influencing stimulation strength. The current amplitude parameter details the current sent through the load (0–100 mA). The Pulse Width (2–20,000 µs) determines the duration of each half cycle, enabling fine control over how the muscle is stimulated. Frequency (20–2000 Hz) specifies the pulse delivery rate, allowing a range of stimulation patterns. Regarding waveforms, three initial options—Ramp-Up Sawtooth, Ramp-Down Sawtooth, and Triangle Sawtooth—use sawtooth signals whose pulse widths are closely tied to the "teeth" time width. A Trapezoidal Sawtooth waveform enables independent adjustment of pulse width, decoupling it from the sawtooth pattern. Additional waveforms—Burst (Single Amplitude), Burst (Increasing Amplitude), and Burst (Increase-Decrease Amplitude)—deliver bursts of pulses, allowing amplitude variation within each burst. The Exponential Increase and Exponential Decrease waveforms follow growth and decay curves, respectively. A Square Wave (Variable Amplitude) option provides direct user control over both amplitude and pulse width. Lastly, variants of the initial sawtooth waveforms grant direct control over pulse width, offering further customisation based on user preferences.

Table 2. Stimulus Parameters Range of Values and Wave Types.

Stimulus Parameters	Range of Values	
Voltage Amplitude (V_{pp})	0 - 50	
Current Amplitude (mA)	0 - 100	
Pulse Width (µs)	2 - 20000	
Frequency (Hz)	20 – 2k	
Wave Type (Biphasic)	1. Ramp-up	7. Burst ramp-down pulse
	2. Ramp-down	8. Burst triangle pulse
	3. Triangle	9. Exponential increase
	4. Trapezoidal	10. Exponential decrease
	5. Burst rectangular pulse	11. Square wave (variable amplitude)
	6. Burst ramp-up pulse	

4.2 Design of Programmable and Flexible Stimulation Waveform

The programmable and flexible stimulation waveform generation system is designed to produce a variety of electrical waveforms based on user-defined parameters. As shown in Figure 5, the system consists of an Arduino microcontroller responsible for waveform control, a digital-to-analogue converter (DAC), and an analogue output stage that shapes and amplifies the signal for functional electrical stimulation (FES). This system enables users to define key stimulus parameters, including amplitude, pulse width, inter-pulse width, frequency, waveform type, and polarity, allowing real-time customization to meet specific neuromuscular rehabilitation needs.

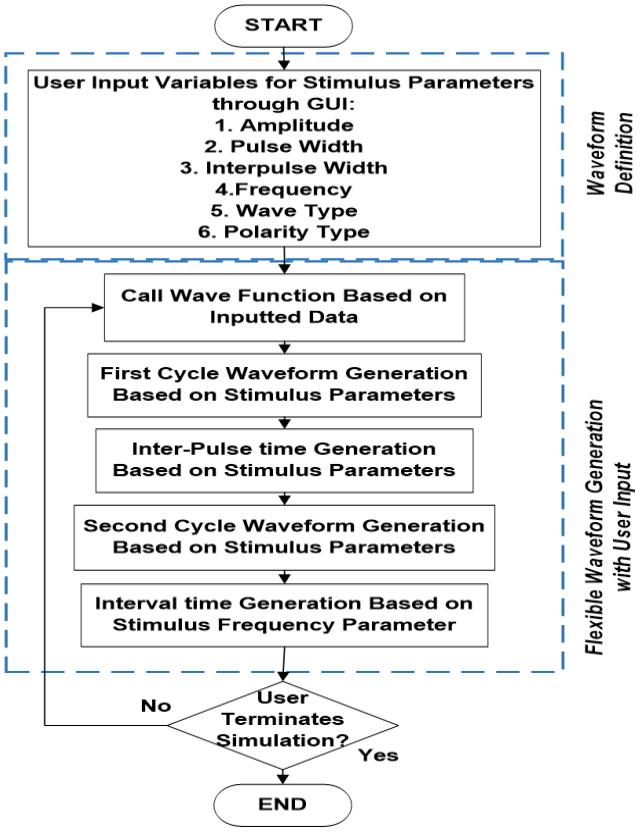

Figure 5: Flexible Waveform Generation Flow.

To ensure precise waveform generation, the system first initializes the hardware, including configuring the DAC and operational amplifier pins. Users input stimulus parameters through a graphical user interface (GUI) [27], which transmits user inputted values to the microcontroller for processing in real time. Based on the user's chosen waveform type, the system calls the corresponding waveform generation function. Each function controls the DAC output and manages waveform characteristics such as rising and falling edges, pulse width, and inter-pulse intervals. The waveform generation process consists of two cycles: the first cycle generates the positive or rising portion of the waveform, while the second cycle generates the negative or falling portion. An inter-pulse interval is inserted between these cycles to ensure proper separation of the positive and negative phases. Additionally, an interval time is introduced at the end of the second cycle to regulate the overall waveform frequency. This process repeats continuously until the user terminates the simulation.

The system supports a diverse range of waveform types, including ramp-up, ramp-down, triangular, trapezoidal, burst pulse, exponential, and square wave, each of which can be configured based on user preferences. This level of programmability allows for customized electrical stimulation, making the system highly flexible for various rehabilitation applications [27].

4.2.1 Flexible Stimulation Waveform Algorithm

The algorithm governing the waveform generation process is detailed in Table 3. The code is structured to ensure maximum flexibility in generating different waveform types based on real-time user

inputs. It begins with hardware initialization, where the setup() function configures the microcontroller's DAC and operational amplifier connections, preparing the system for waveform output.

User-defined parameters play a central role in waveform customization. The system allows users to input values such as amplitude, pulse width, inter-pulse width, frequency, waveform type, and polarity via the GUI. These parameters directly influence the shape and properties of the generated waveform, enabling precise control over electrical stimulation.

To accommodate different waveform types, the code includes dedicated waveform generation functions, each responsible for producing a specific pattern. These functions adjust the DAC output and regulate waveform timing to achieve the desired shape and amplitude. A continuous looping mechanism within the loop() function ensures that the system maintains uninterrupted waveform generation based on the selected user parameters.

The algorithm follows a structured flow, beginning with checking user inputs and selecting the appropriate waveform function. The system then executes a first cycle to generate the waveform's initial phase, applies inter-pulse timing to maintain proper separation between phases, and proceeds with a second cycle to complete the waveform. Finally, an interval time is introduced to control frequency, and the loop repeats until the user stops the simulation.

Table 3. Programmable and Flexible Waveform Generation Algorithm.

Algorithm 1. Programmable and Flexbile Waveform Generation

1. START
2. Define Port A for DAC Output
3. Define Port B for Stimulus waveform output polarity
4. Define Stimulus Parameters: Wavetype, amplitude, pulse width, interpulse width, frequency, polarity
5. Loop: Check wavetype choise and stimulus parameters:
6. if Wavetype choice is Rectangular; Call Rectangular function
7. else if Wavetype choice is Ramp-up; Call Ramp-up function
8. else if Wavetype choice is Ramp-down; Call Ramp-down function
9. else if Wavetype choice is Triangle; Call Triangle function
10. else if Wavetype choice is Trapezoidal; Call Trapezoidal function
11. else if Wavetype choice is Burst rectangular pulse; Call Burst rectangular pulse function
12. else if Wavetype choice is Burst ramp-up pulse; Call Burst ramp-up pulse function
13. else if Wavetype choice is Burst ramp-down pulse; Call Burst ramp-down pulse function
14. else if Wavetype choice is Burst triangle pulse; Call Burst triangle pulse function
15. else if Wavetype choice is Exponential increase pulse; Call Exponential increase pulse function
16. else if Wavetype choice is Exponential decrease pulse; Call Exponential decrease pulse function
17. First cycle waveform generation based on stimulus parameter settings
18. Inter-pulse time generation based on stimulus parameter settings
19. Second cycle waveform generation based on stimulus parameter settings
20. Interval time generation based on stimulus frequency parameter settings
21. User terminates simulation?
22. If NO, goto Loop (continue looping)
23. If YES, END

4.2.2 Integration of GUI with the Microcontroller

The GUI serves as the primary interface for users to input waveform parameters and interact with the Arduino-based stimulator. It transmits data to the Arduino via serial communication, enabling seamless integration between software and hardware. Upon receiving data, the Arduino parses the input string, extracts waveform parameters, and assigns them to their respective variables. Based on the selected waveform type, the appropriate function is executed, ensuring the generated waveform aligns with user specifications. This process allows real-time parameter adjustments without requiring a system restart.

As shown in Figure 6, the GUI provides an intuitive platform for waveform selection and parameter configuration. Users can choose from a dropdown menu of waveform types, with real-time graphical updates reflecting their selection. Input fields dynamically adjust based on the chosen waveform, ensuring only relevant parameters are displayed. Once configured, waveform parameters are transmitted to the Arduino via a "Send to Arduino" button, where they are processed and applied to the stimulator.

International Journal of Environmental Sciences
ISSN: 2229-7359
Vol. 11 No. 21s, 2025
https://theaspd.com/index.php

For an in-depth discussion on the GUI implementation, communication protocol, and its integration with the Arduino, refer to [27]. The combination of a user-friendly interface and real-time programmability enhances the system's efficiency, making it a versatile tool for neuromuscular rehabilitation and experimental bioelectrical applications.

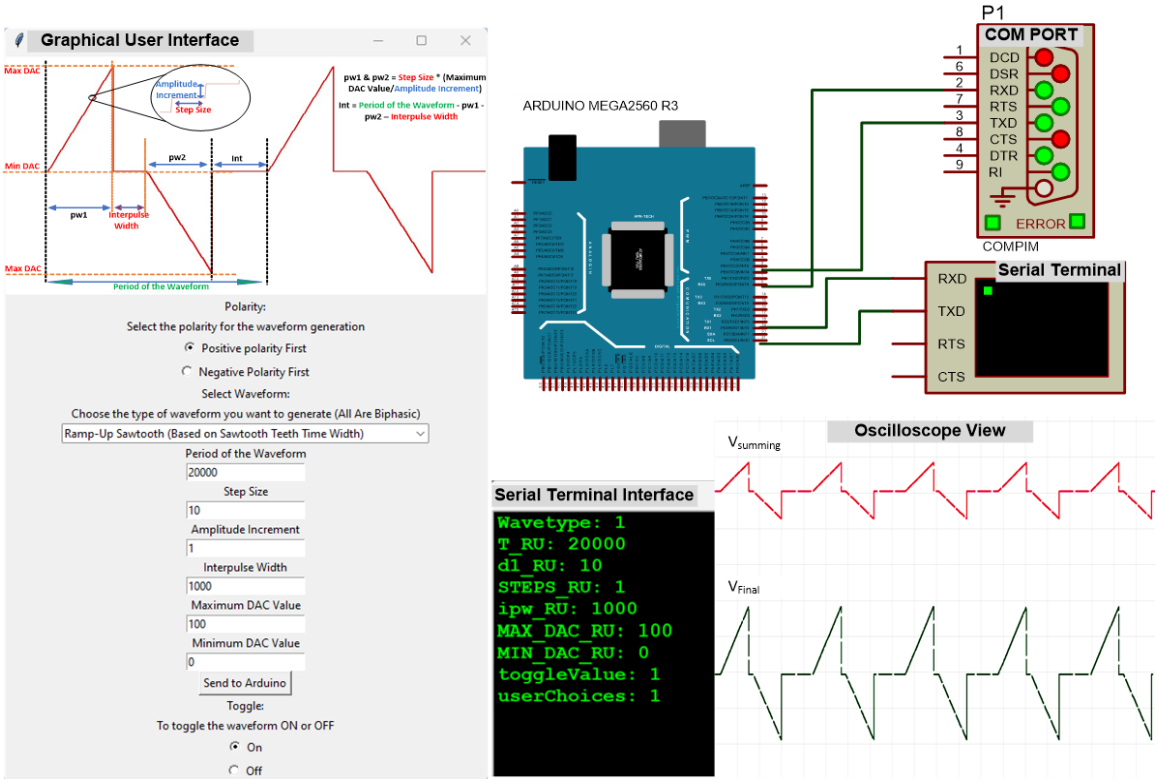

Figure 6: Full view of GUI and Arduino functionality [27].

4.3 Design and Simulation of the Biphasic Output Current Source Circuit

As shown in Figure 7, the complete biphasic output circuit was replicated and simulated using Proteus to verify correct timing, gain, and polarity transitions. This schematic directly corresponds to the design principles depicted in Figure 3, including the non-inverting, inverting, summing, and Improved Howland Charge Pump amplifiers. A 5 V pulse source was applied to both the inverting and non-inverting inputs (with user chosen offset on the inverting side) to emulate the programmed signals from the DAC. Through simulations, each op-amp stage behaved as expected, maintaining the biphasic signal integrity and delivering stable current at the final output node. Simulated waveforms confirmed that the circuit equations (1)–(3) were satisfied, producing matching results to those anticipated in the theoretical design.

Hence, Figure 7 validates the functional equivalence between the Proteus schematic and the conceptual circuit in Figure 3, underscoring that the biphasic output stages perform consistently under practical simulated conditions.

4.4 Implementation of Programmable and Flexible Stimulation Waveform using Biphasic Output Current Source Circuit in Proteus

The basic biphasic output current source circuit is implemented as a programmable circuit where the output current of the biphasic circuit can be varied according to the interface received from the GUI, as illustrated in Figure 6. The complete programmable biphasic circuit implementation is shown in Figure 7, where the DAC signals feed into non-inverting and inverting amplifier stages and ultimately pass through an improved Howland charge pump. The microcontroller and GUI interface allow users to define key stimulation parameters—such as amplitude, frequency, and polarity—which the circuit then translates into precisely timed positive and negative pulses. As detailed in Table 1, the design utilizes a 74HC4016 switch for phase control, LM 741 operational amplifiers for initial signal conditioning, and an OPA454 high-current amplifier to handle higher output loads. The listed resistor values set gain factors and ensure stable current delivery, while the load resistor can be swapped out (e.g., 500 Ω, 1 kΩ, or 2 kΩ) to accommodate different rehabilitative requirements.

International Journal of Environmental Sciences
ISSN: 2229-7359
Vol. 11 No. 21s, 2025
https://theaspd.com/index.php

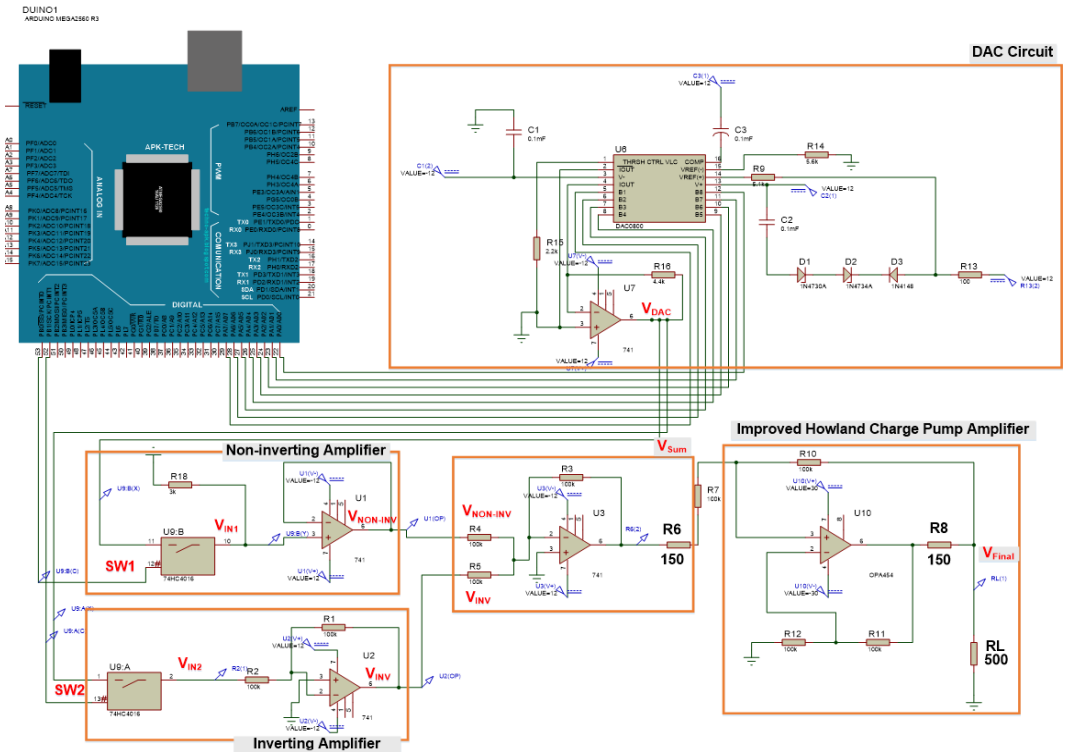

Figure 7: Overall circuit of the programmable biphasic circuit.

4.5 Hardware Measurement Setup

The hardware measurement setup, illustrated in Figure 8, integrates multiple components for comprehensive FES system testing. A graphical user interface (GUI) displayed on a computer monitor enables user control and parameter configuration, interfacing with an Arduino Mega 2560 microcontroller as the main control unit. The signal chain includes a DAC 0800 for digital-to-analogue conversion, 74HC4016 switching logic circuits, and inverting/non-inverting operational amplifier circuits for waveform conditioning. An Improved Howland circuit provides the final stage of current control and signal amplification. A digital oscilloscope is used for real-time waveform visualization and measurement. All components are assembled on a breadboard, facilitating rapid prototyping and detailed testing of the system's ability to produce controlled stimulation waveforms.

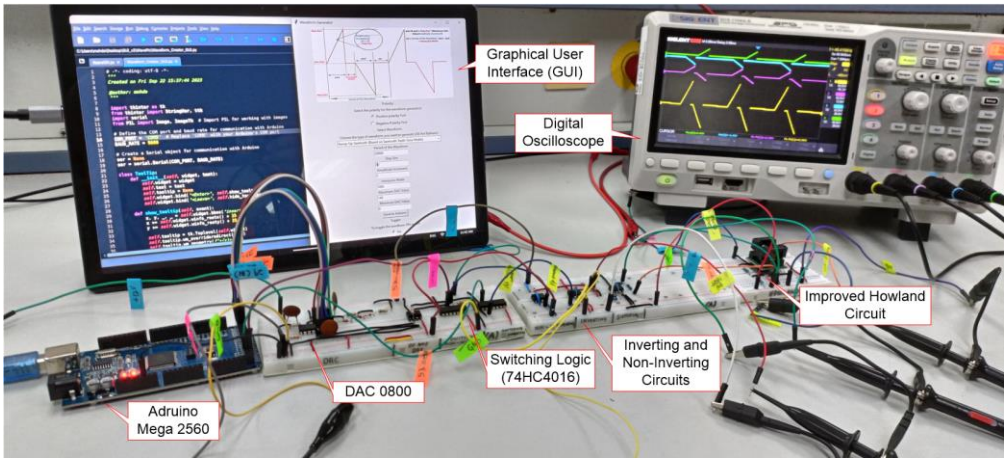

Figure 8: Hardware measurement setup.

5 RESULTS AND DISCUSSION

This section presents both the simulation and hardware measurement outcomes, providing a comprehensive evaluation of the programmable biphasic waveform stimulator. The initial subsection discusses results obtained via Proteus simulation, confirming that the design meets essential performance criteria and offers a high degree of programmability. The subsequent subsection focuses on the hardware measurements, which validate the stimulator's real-world functionality through oscilloscope captures

5.1 Proteus Simulation

The Proteus simulation results validate the functionality and flexibility of the programmable waveform stimulator. Figure 9 demonstrates the system's programmability through two implementations of the Ramp-Up waveform with significantly different parameters. Figure 9(a) shows a high-frequency configuration with a period of 300 µs, step size of 5 µs, and interpulse width of 100 µs, producing a $28V_{pp}$ output. The DAC values range from 0 to 100 units with a step increment of 10 units, resulting in precise waveform generation at microsecond timescales.

In contrast, Figure 9(b) demonstrates the system's capability to generate larger amplitude, slower waveforms with a period of 550,000 µs, step size of 20,000 µs, and interpulse width of 10,000 µs, producing a $60V_{pp}$ output. This configuration utilizes the full DAC range (0-255 units) with a step increment of 20 units. Polarity control is demonstrated by initiating the waveform with the negative phase, showcasing the system's programmable phase selection capability.

The system's versatility in generating diverse waveform patterns is further illustrated in Figure 10, which displays the complete range of implemented waveforms. These include waveforms as listed in Table 2. Each waveform maintains precise timing relationships and proper biphasic symmetry, demonstrating the system's capability to produce complex stimulation patterns while maintaining waveform fidelity.

The digital oscilloscope traces confirm consistent waveform characteristics across multiple cycles, with clean transitions and stable amplitude levels. The simulation results validate that the improved Howland charge pump circuit effectively generates the required output waveforms across the full range of programmed parameters. The system successfully demonstrates the capability to generate both rapid, low-amplitude stimulations and slower, high-amplitude patterns, providing the flexibility needed for various FES applications.

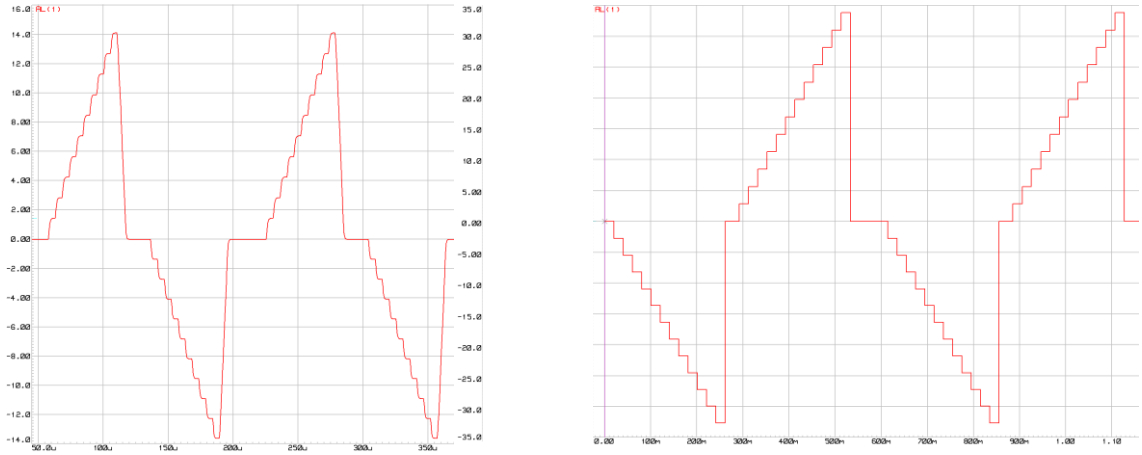

(a) (b)

Figure 9: Proteus simulation results demonstrating timing and amplitude programmability: (a) Ramp-Up waveform with $28V_{pp}$ amplitude, 300 µs period, and positive-first polarity; (b) Ramp-Up waveform with $60V_{pp}$ amplitude, 550,000 µs period, and negative-first polar.

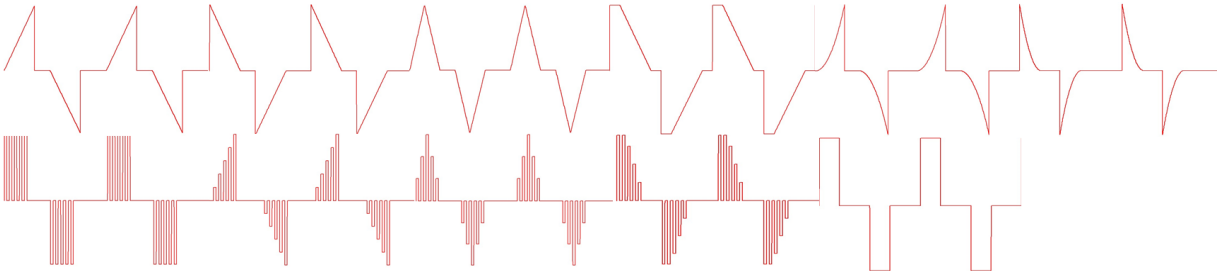

Figure 10: Complete set of programmable waveform patterns implemented in the system, showing (from top to bottom) Ramp-Down, Triangle, Trapezoidal, Burst patterns, Exponential, and Rectangular waveforms.

5.2 Hardware Measurement

This section details the hardware measurements conducted to validate the functionality of the programmable biphasic waveform stimulator. Each subsection focuses on a specific aspect of the system: the

DAC output, overall circuit functionality, flexible waveform generation, timing/amplitude resolution, and a brief comparative analysis.

5.2.1 DAC Output Waveform

To verify the digital-to-analogue converter (DAC) behaviour, the Arduino microcontroller was configured to output a ramp-up pattern ranging from 0 to 255 in DAC units. The main objective was to observe the linearity of the DAC output when translating digital codes into analogue voltage steps [14]. A maximum code of 255 corresponds to the highest DAC output level, while 0 produces a baseline level near 0 V. DAC measurements were taken at V_{DAC} as seen in Figure 7.

Figure 11(a) shows an overview of this ramp-up waveform with a 20 ms interval between each cycle. The captured oscilloscope trace reveals a steadily ascending slope, confirming that the DAC delivers incremental voltage steps. Figure 11(b) provides a zoomed-in view (marked area B), illustrating the consistent gap between steps, indicative of linear behaviour. This linear output is crucial for subsequent amplifier stages, as it ensures accurate voltage-to-current conversion in the biphasic circuitry.

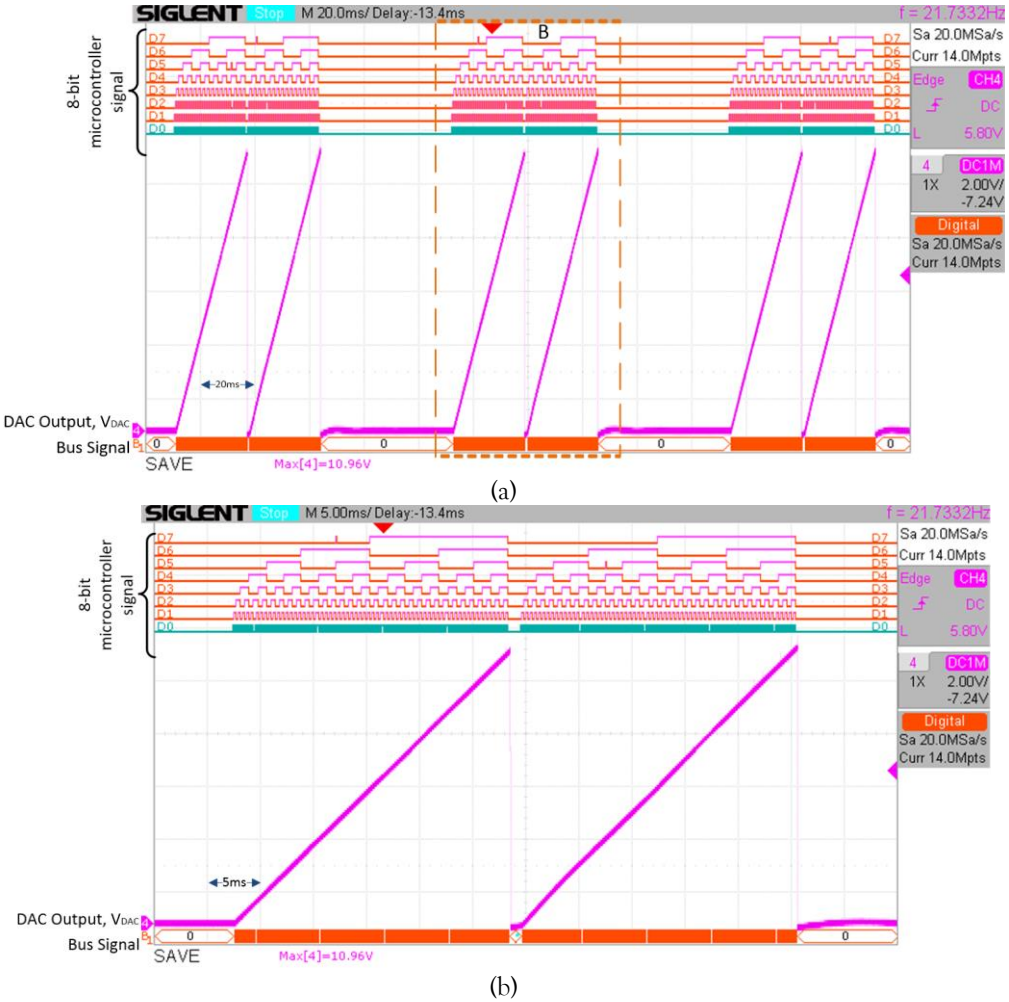

Figure 11: DAC waveform output set to Ramp Up at Maximum DAC value of 255: (a) Overview of waveform every 20 ms; (b) Zoom view into marked area B.

5.2.2 Overall Circuit Functionality: Inverting, Non-Inverting, and Howland Outputs

After verifying the DAC output, the signals were routed to the non-inverting, inverting, summing, and Howland charge pump stages to form a complete biphasic stimulator. The aim was to demonstrate proper phase control, amplitude handling, and current-mode operation. Figures 12 and 13 present oscilloscope captures of four signals.

Figure 12 illustrates a ramp up waveform, captured at a 5 ms/div timescale. The pink trace ($V_{NON\text{-}INV}$) transitions from a lower voltage to a higher voltage in a gradual "ramp-up" fashion, while the red trace (V_{INV}) shifts inversely, indicating the 180° phase shift from the inverting amplifier. The green summation signal

(V_{SUM}) slopes upward in tandem with $V_{NON-INV}$, offset by the negative contribution from V_{INV}. Finally, the blue trace (V_{Final}) shows the result of the Howland charge pump converting V_{SUM} into a stable current output, achieving a peak-to-peak amplitude of around 43 V. This confirms that the biphasic transitions remain smooth and well-separated in time, avoiding overlaps between positive and negative phases.

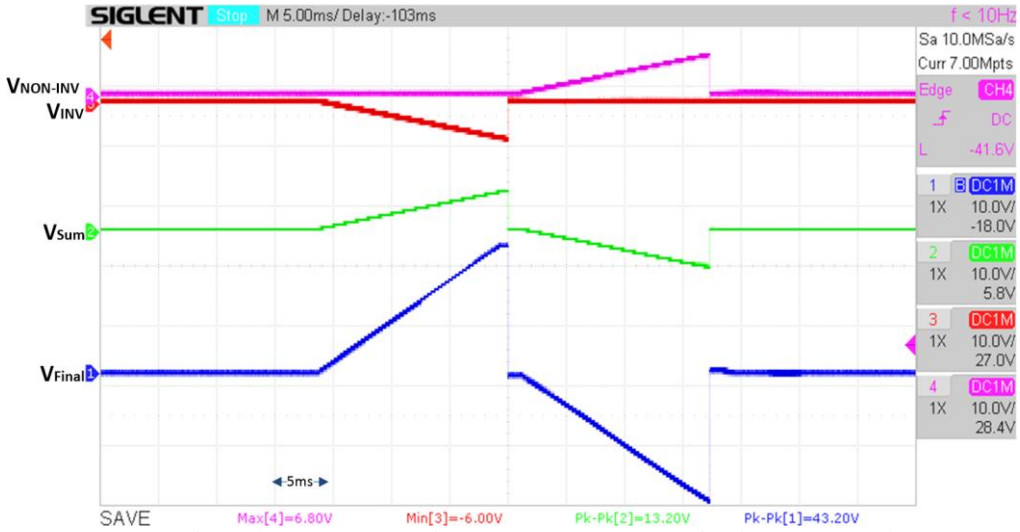

Figure 12: Ramp up waveform showing outputs from non-inverting amplifier ($V_{NON-INV}$, pink), inverting amplifier (V_{INV}, red), summing amplifier (V_{SUM}, green), and final output (V_{Final}, blue).

Figure 13 uses a 500 µs/div scale and exhibits a rectangular waveform. The pink and red traces indicate that $V_{NON-INV}$ and V_{INV} each hold relatively constant levels for part of the cycle, then quickly switch polarity. The green summation node (V_{SUM}) accordingly toggles between positive and negative voltages, creating a near-ideal ± rectangle at the summing amplifier output. The blue trace (V_{Final}) reaches a peak-to-peak amplitude of about 45 V, confirming that the Howland stage provides robust final amplification and symmetrical biphasic behaviour. Notably, even at these faster transitions, distortion is minimal, reflecting a properly configured op amp network.

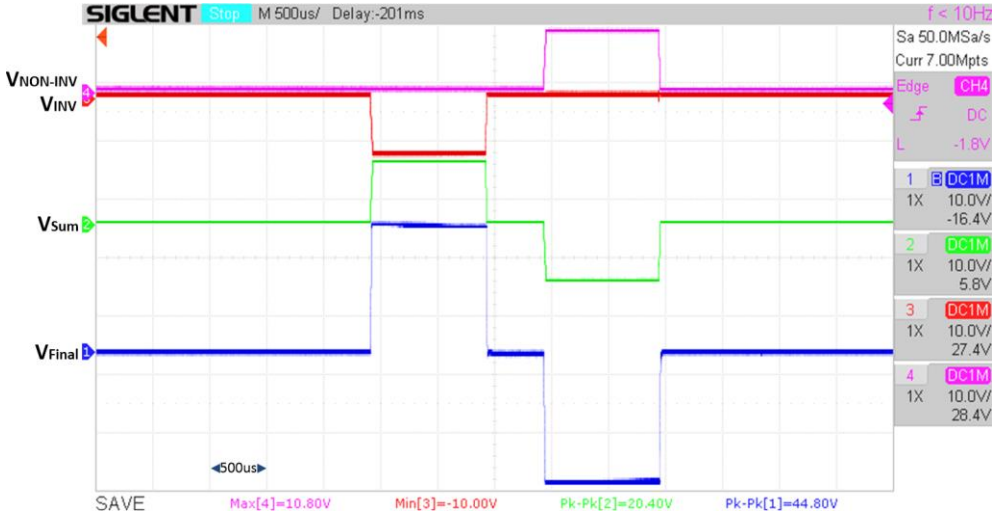

Figure 13: Rectangle waveform showing outputs from non-inverting amplifier ($V_{NON-INV}$, pink), inverting amplifier (V_{INV}, red), summing amplifier (V_{SUM}, green), and final output (V_{Final}, blue).

5.2.3 Measured Flexible Output Waveforms

This section presents oscilloscope captures for the diverse biphasic waveforms generated by the stimulator at its final output stage, grouped according to basic biphasic, exponential, rectangular, and burst-type shapes. Each waveform was configured via the graphical user interface to demonstrate varying slopes, durations, and amplitudes, with peak outputs measured up to ±50 V. The pulse durations are configurable from 2 µs to 20 ms, offering both fine temporal resolution and flexibility for different neuromuscular stimulation needs.

Table 4 summarizes the four waveform groups, referencing Figures 14–16, where each figure is shown as a composite with sub-figure labels (a), (b), and so on for the specific waveforms within that group.

Table 4. Overview of Measured Flexible Output Waveforms (Figures 14–16).

Waveform Group	Figure	Included Waveforms	Key Characteristics
Rectangular	14	Rectangular pulse	- Sharp transitions between positive and negative phases
Flexible Shapes	15	(a) Ramp Up (b) Ramp Down	- Ramp Up: Smooth ascending slope with negative return - Ramp Down: Smooth descending slope with negative return
		(c) Exponential Up (d) Exponential Down	- Gradual, nonlinear slope changes - "Up" variant increases before negative phase - "Down" variant decreases before negative phase
		(e) Triangle (f) Trapezoidal	- Triangle: Symmetrical rising and falling edges - Trapezoidal: Extended plateau at peak amplitude
Burst-Type	16	(a) Burst Pulse (b) Ramp Up Burst Pulse (c) Ramp Down Burst Pulse (d) Triangle Ramp Burst Pulse	- Multiple pulses grouped in each biphasic cycle - May incorporate ascending or descending slopes, or triangular patterns within each burst

1. Basic Rectangular Biphasic Waveform

While rectangular biphasic waveforms are not ideal for controlled muscle fatigue management due to their abrupt transitions, the stimulator retains the ability to generate them when necessary. This ensures compatibility with conventional FES while providing full programmability through a graphical user interface (GUI). Figure 14 presents the measured output waveforms, demonstrating real-time parameter adjustability.

In Figure 14(a), the waveform operates at 50 Hz, with the DAC output set to 255 for both the positive and negative pulse widths, ensuring equal amplitude in both directions. The first and second pulse width durations were each set to 1000 µs, defining how long each pulse width lasted before switching polarity. An interpulse width (I_{PW}) of 500 µs introduced a brief delay between biphasic cycles. The measured peak-to-peak output voltage (P_k- P_k) was 45.2 V, and with a 500 Ω load resistance, the corresponding stimulation current was 90.4 mA.

In Figure 14(b), the frequency was increased to 100 Hz, while DAC value was reduced to 200 to decrease the pulse amplitude. The I_{PW} remained at 500 µs, but both positive and negative pulse widths were extended to 2000 µs to provide a longer, more sustained pulse width. The measured P_k- P_k voltage was 44.8 V, leading to a calculated current of 89.6 mA with the same 500 Ω load resistance.

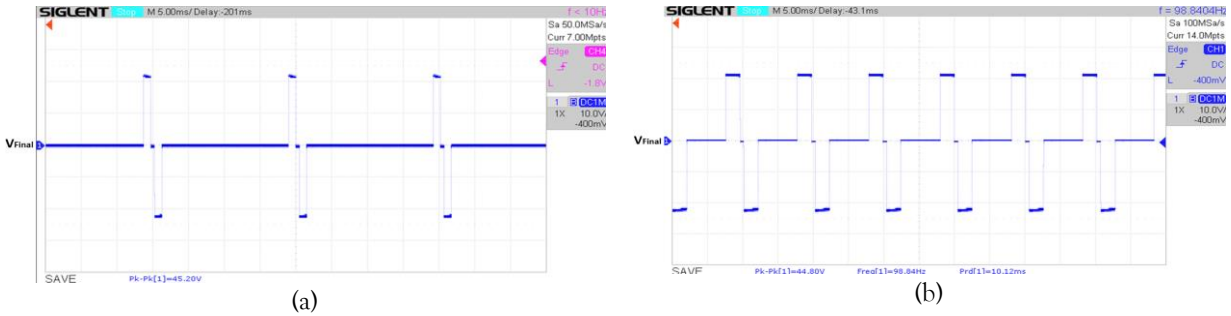

Figure 14: Measured rectangular biphasic waveforms at (a) 50 Hz with 45.2V_{pp} output and (b) 100 Hz with 44.8V_{pp} output. Both waveforms were generated using the programmable stimulator with a 500 Ω load.

This stimulator provides full control over amplitude, frequency, and pulse width durations, enabling customized neuromuscular activation patterns. Unlike conventional FES devices with fixed parameters, this system allows real-time adjustments, ensuring flexibility for various applications, including neuromuscular rehabilitation, and muscle training.

International Journal of Environmental Sciences
ISSN: 2229-7359
Vol. 11 No. 21s, 2025
https://theaspd.com/index.php

2. Flexible Shape Biphasic Waveform

Figure 15 demonstrates the stimulator's ability to generate a wide range of biphasic waveforms with real-time parameter adjustments via a GUI. Unlike conventional stimulators limited to rectangular pulses, this system allows customization of waveform shape, amplitude, pulse width, and interpulse interval transition durations, enhancing its suitability for neuromuscular rehabilitation and experimental applications. Supported waveforms include ramp-up, ramp-down, exponential increase, exponential decrease, triangular, and trapezoidal, all ensuring charge-balanced stimulation. The ramp-up waveform in Figure 15(a) gradually increases amplitude with each tooth before polarity reversal. Generated at 20 Hz with a DAC output of 150, an I_{PW} of 500 µs, and a step increment of 1 every 30 µs, it achieved a Pk-Pk voltage of 41.6 V, yielding a 83.2 mA stimulation current. The ramp-down waveform in Figure 15(b) follows the opposite pattern, decreasing amplitude with each tooth. At 50 Hz, with a DAC output of 140, an I_{PW} of 500 µs, and a step decrement of 1 every 30 µs, it produced a Pk-Pk voltage of 43.2 V and a stimulation current of 86.4 mA. The exponential increase waveform in Figure 15(c) follows a nonlinear progression, starting gradually and accelerating toward the peak. Configured at 50 Hz with a DAC output of 140, an I_{PW} of 1000 µs, and 100 steps over 6000 µs, it resulted in a Pk-Pk voltage of 42.4 V and a stimulation current of 84.8 mA. The exponential decrease waveform in Figure 15(d) exhibits the inverse pattern, with a rapid initial drop that slows toward the end of each half-wave. At 50 Hz, with a DAC output of 120, an I_{PW} of 2000 µs, and 100 steps over 6000 µs, it generated a Pk-Pk voltage of 41.6 V and a stimulation current of 83.2 mA. The triangular waveform in Figure 15(e) features a linear increase and decrease within each half-wave. Configured at 50 Hz with a DAC output of 140, an I_{PW} of 1000 µs, and a step increment of 1 every 15 µs, it produced a Pk-Pk voltage of 42.8 V and a stimulation current of 85.6 mA. The trapezoidal waveform in Figure 15(f) maintains a sustained peak amplitude before polarity transition, blending rectangular and triangular characteristics. At 50 Hz with a DAC output of 140, an I_{PW} of 1000 µs, and a plateau duration of 1000 µs, it resulted in a Pk-Pk voltage of 42.4 V and a stimulation current of 84.8 mA. By enabling diverse waveform generation with fine-tuned real-time control, the stimulator surpasses conventional FES devices with fixed profiles. This flexibility optimizes rehabilitation protocols, reduces muscle fatigue, and enhances precision in neuromuscular stimulation and bioelectrical research.

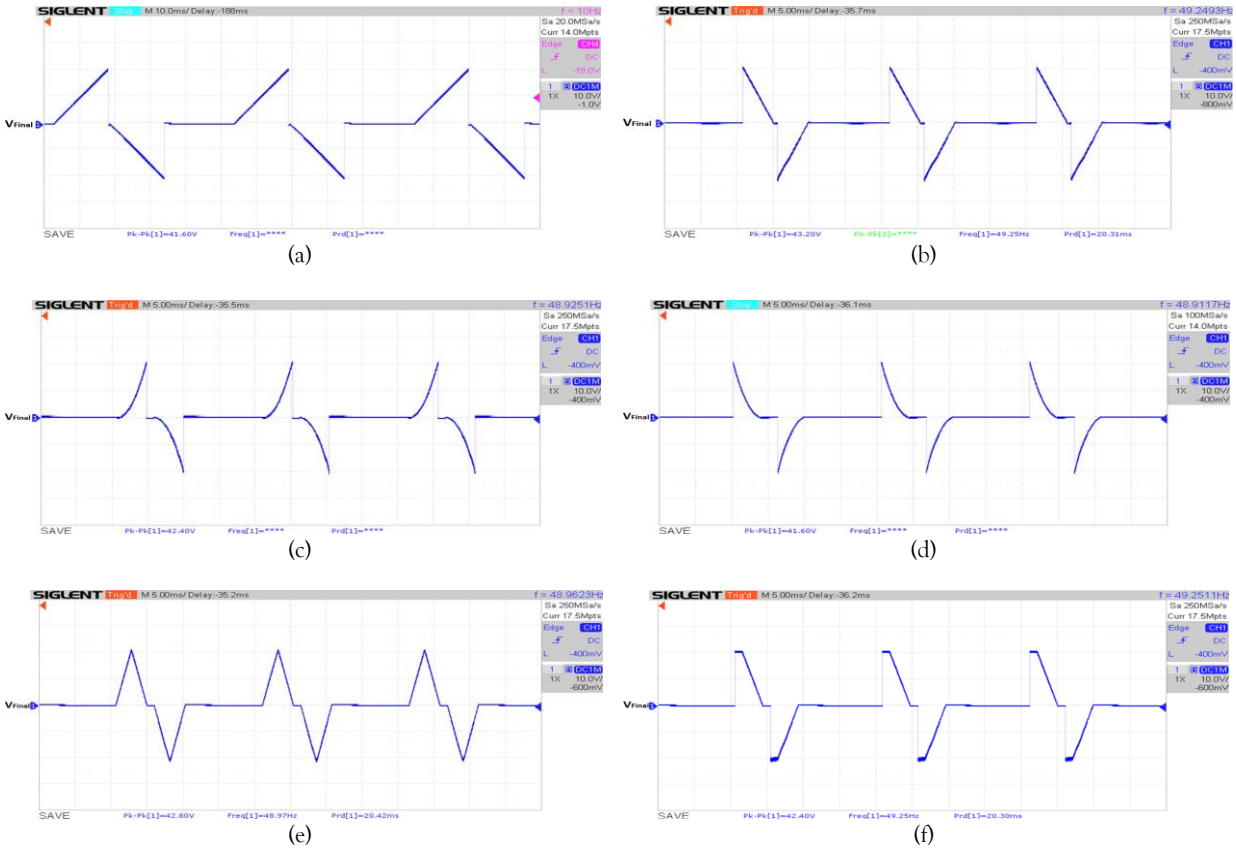

Figure 15: Composite of flexible shape biphasic output waveforms (final output): (a) Ramp-up, (b) Ramp-down, (c) Exponential increase, (d) Exponential decrease, (e) Triangular, and (f) Trapezoidal waveforms.

3. Burst Waveform

As seen in Figure 16, the stimulator supports burst-mode biphasic stimulation, where multiple pulses are grouped into rapid sequences before an interpulse interval. This allows fine-tuned neuromuscular recruitment and fatigue management. Unlike conventional fixed-frequency stimulators, the burst mode permits custom pulse counts, durations, and delays, enabling personalized stimulation protocols.

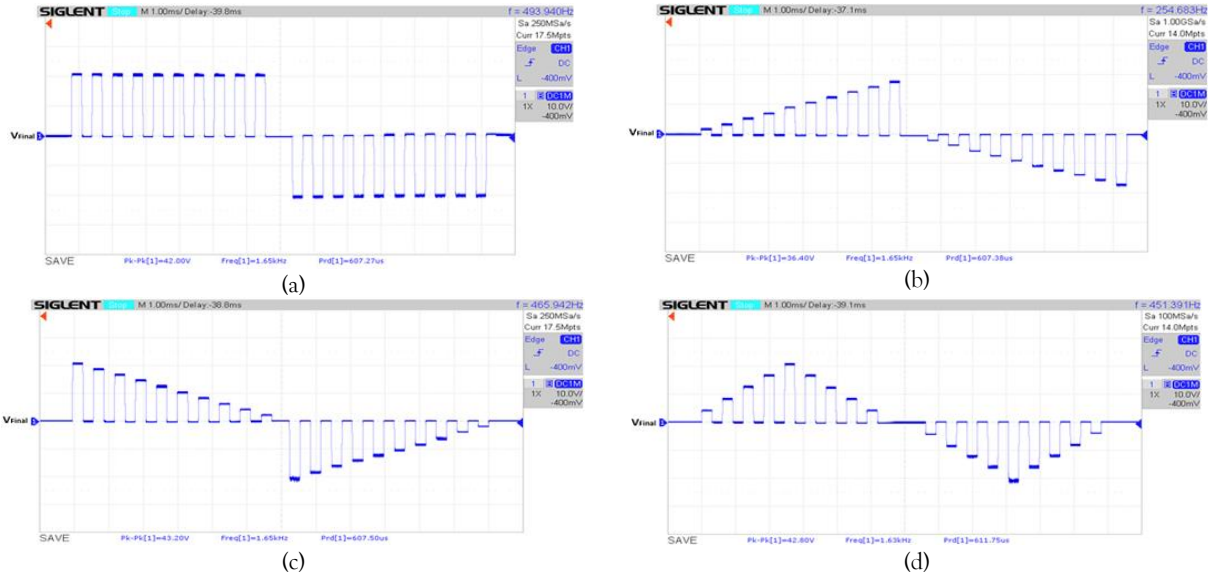

Figure 16: Composite burst-type waveforms measured at the final output stage: (a) Burst pulse waveform, (b) Ramp up burst pulse waveform, (c) Ramp down burst pulse waveform, (d) Triangle ramp burst pulse waveform.

The burst pulse waveform in Figure **16**(a) consists of evenly spaced pulses grouped within bursts. It was generated at 50 Hz, with 10 pulses per burst, a pulse duration of 300 µs, and an inter-burst delay of 300 µs. The DAC output was 140, producing a P_k- P_k voltage of 42.00 V, resulting in a stimulation current of 84.00 mA with a 500 Ω load. **The ramp-up burst waveform in** Figure **16**(b) gradually increases amplitude within each burst. With the same 50 Hz frequency and burst settings, the ramping effect reduced the P_k- P_k voltage to 36.40 V, leading to a stimulation current of 72.80 mA. **The ramp-down burst waveform** in Figure **16**(c) follows the inverse pattern, with amplitude decreasing within the burst. It was configured identically, but the P_k- P_k voltage measured 43.20 V, producing a stimulation current of 86.40 mA. **The triangular ramp burst waveform in** Figure **16**(d) modulates amplitude symmetrically within each burst. With identical settings, the P_k- P_k voltage was 42.80 V, leading to a stimulation current of 85.60 mA.

This programmable and flexible burst stimulation mode enables progressive or varying intensity bursts, reducing muscle fatigue and optimizing stimulation strategies. Unlike conventional stimulators with fixed burst patterns, this system dynamically modulates burst intensity in real-time, enhancing neuromuscular rehabilitation and research applications.

5.2.4 Timing and Amplitude Resolution (LSB Analysis)

Figure 17, shows that the FES protocol can have a resolution of 2 µs. Compared to previous research, this design improves timing resolution. The FPGA-based stimulator by Mercado-Gutierrez et al. [14] achieves a pulse width range of 20–400 µs with high linearity and repeatability. However, the minimum timing step size is not explicitly defined. If the system only allows pulse width increments of 20 µs or greater, its fine-tuning capability is limited. The ESP32-based system by Basumatary et al. [27] offers 5–500 µs pulse width resolution, but it relies on a 12.5 mV DAC step, making it less precise for low-amplitude adjustments. Additionally, its use of a step-up transformer introduces electromagnetic interference (EMI) concerns, potentially affecting stability.

The 2 µs timing resolution of this stimulator surpasses both designs, offering superior flexibility in defining stimulation patterns, particularly for progressive amplitude increases, complex modulation schemes, and fatigue-reducing protocols. This level of precision enhances its suitability for neuromuscular rehabilitation, where small parameter variations can significantly influence motor responses.

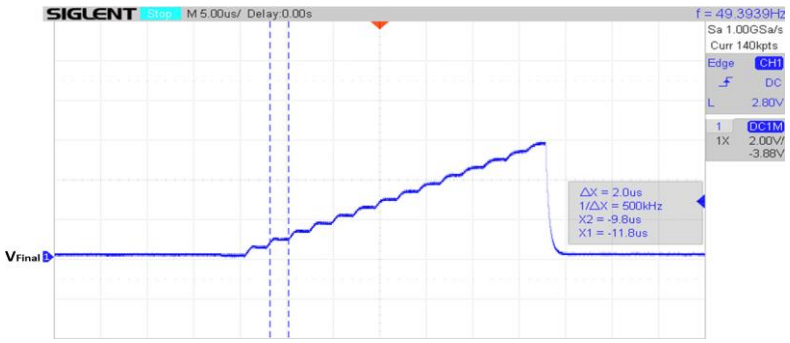

Figure 17: Evidence that resolution can be as low as 2µs.

5.2.5 Comparative Analysis

The developed programmable and flexible stimulator is compared with existing functional electrical stimulation (FES) systems to evaluate its advantages in controller complexity, biphasic circuit design, stimulus parameters, and waveform flexibility. Table 5 provides an overview of various hardware-based FES implementations, highlighting differences in architecture, output capabilities, and design trade-offs.

Table 5. Comparative Analysis of FES Stimulator Designs.

Ref	Controller	Waveform Types	Frequency	Pulse Width	Output	Key Features
[8]	Custom low-cost hardware	Biphasic rectangular pulses	20-50 Hz (fixed)	100-500 µs	Up to ~46 V (tested at ~12-15 V)	Cost-effective 3 V supply with H-bridge & boost; safer but limited waveform variety
[26]	STM32-based embedded system	Biphasic trapezoidal, ramp-up/down	10-50 Hz	20-500 µs	Up to 50 V	Enhanced reliability vs. inertial-sensor approaches; limited clinical validation
[14]	FPGA (Spartan R-6 XC6SLX9-2TQG144I)	Biphasic rectangular	1-150 Hz	20-400 µs (Resolution of 10 µs)	Up to 50 V; 1-48 mA	High linearity, repeatability, flexible parameter control, scalable to multiple channels
[28]	ESP32 microcontroller	Biphasic trapezoidal (generated from rectangular pulses)	10-100 Hz	5-500 µs	Up to 200 V_{pp}	Low-cost with adjustable parameters; higher amplitude but bulky transformer-based design
[29]	External remote microcontroller	Biphasic rectangular	1-100 Hz	Not specified	1.2V and 3V 0.336-1.51 mA	Programmable FES architecture with flexible stimulus levels; external controller may hinder usability
[30]	NUCLEO-L432KC microcontroller	Biphasic rectangular pulse	0-1 kHz	50 µs -1000 µs	50 µA-1 mA	Precisely adjustable multi-lead outputs; targeted for in vitro research setups
This Work	Arduino Mega 2560 + Hardware + GUI	Biphasic ramp-up/down, triangle, trapezoidal, burst pulses, exponential (up/down), square wave	20 Hz-2 kHz	2-20,000 µs	±50 V, ±100 mA	High-voltage capacity with broad waveform range; real-time parameter tuning via GUI; validated by hardware

Studies, such as those by Mercado-Gutierrez et al. [14] and Fenko et al. [30], employ an FPGA or high-performance microcontrollers such as the NUCLEO-L432KC, which provide precise waveform generation but at the cost of increased circuit complexity and higher development costs. Similarly, Bakhtina et al. [26] utilized an STM32-based system, which offers improved reliability but remains limited in its flexibility. In contrast, this work adopts an Arduino Mega 2560, a cost-effective and widely available microcontroller that simplifies hardware implementation while retaining high-resolution control over waveform parameters. Unlike FPGA-based designs, which require complex programming and additional hardware integration, the Arduino-based approach facilitates real-time adjustments via an intuitive graphical user interface (GUI), reducing setup time and system complexity without compromising performance.

FES output circuits vary in complexity, often impacting the ability to generate flexible stimulation waveforms. Many systems, including those by Basumatary et al. [28] and Kumar et al. [29], employ external transformers or remote microcontrollers to shape pulse characteristics, increasing design bulk and susceptibility to electromagnetic interference (EMI). Other designs, such as Mercado-Gutierrez et al. [14], implement specialized circuits optimized for fixed biphasic rectangular pulses, limiting flexibility. The proposed stimulator in this work integrates a simplified yet versatile biphasic circuit composed of a DAC-driven analogue output stage and an improved Howland charge pump amplifier. This compact implementation enables the generation of diverse waveforms, including ramping, exponential, and burst pulses, without requiring additional hardware or high-power transformers. Compared to FPGA- or transformer-based systems, this circuit minimizes board space, reduces EMI risks, and maintains efficient current delivery for neuromuscular rehabilitation applications.

FES efficacy depends on its stimulus parameters, including frequency range, pulse width, and output amplitude. Systems such as Stewart et al. [8] and Bakhtina et al. [26] support relatively narrow frequency and pulse width ranges (20–50 Hz, 100–500 μs), making them suitable for specific applications but less flexible to varying neuromuscular conditions. Meanwhile, FPGA-based and microcontroller-controlled devices such as those by Mercado-Gutierrez et al. [14] and Basumatary et al. [28] offer expanded parameter tuning but with constraints on waveform diversity and real-time modification. This work surpasses previous designs by delivering an extensive parameter range: frequency modulation from 20 Hz to 2 kHz and pulse width adjustability from 2 μs to 20,000 μs. This broad configuration enables a more precise tuning of stimulation intensity and duration, accommodating a wider spectrum of rehabilitation protocols. Additionally, the ±50 V and 100 mA peak output capacity allows for both low-intensity and high-amplitude stimulation, making the system highly flexible to various neuromuscular applications.

Most existing FES systems, such as Stewart et al. [8], Kumar et al. [29], and Fenko et al. [30], rely primarily on biphasic rectangular pulses, limiting their flexibility for advanced stimulation protocols. Although some designs, such as Bakhtina et al. [26] and Basumatary et al. [28], incorporate trapezoidal and ramping pulses, they often require specialized circuit modifications or additional processing components to generate these waveforms. The developed stimulator introduces a comprehensive set of waveform options, including ramp-up/down, triangle, trapezoidal, burst pulses, and exponential (up/down) patterns, in addition to biphasic rectangular pulses. Unlike previous designs that require manual hardware reconfiguration, the GUI-based interface allows real-time selection and parameter tuning of these waveforms. This flexibility enhances its applicability in neuromuscular rehabilitation, fatigue-resistant stimulation, and research applications requiring programmable and flexible waveform modulation.

This work presents a programmable and highly flexible FES stimulator that addresses key limitations of existing designs. By leveraging a cost-effective microcontroller, a simplified yet versatile biphasic output circuit, and an extensive range of stimulus parameters, the system provides a superior alternative to FPGA- and transformer-based implementations. Its ability to generate multiple waveform types, combined with real-time tunability via a GUI, makes it a practical and efficient solution for a wide range of neuromuscular rehabilitation and research applications.

6 CONCLUSION

This research has successfully developed and validated a programmable biphasic waveform stimulator for FES applications, integrating a user-friendly graphical interface for intuitive control. The system demonstrates precise generation of multiple waveform patterns—including ramp, trapezoidal, triangular, exponential, rectangular, and burst configurations—with accurate control of current (0-100 mA), pulse width (2-20000 μs), and frequency (20-2000 Hz). Comprehensive validation through both Proteus simulation and hardware measurements confirms reliable reproduction of programmed waveforms with consistent timing and amplitude characteristics. The system addresses fundamental limitations of conventional FES devices by providing flexible stimulation patterns that can be tailored to individual rehabilitative needs. Notably, the successful implementation of ramp and triangular patterns aligns with research suggesting improved muscle fatigue management through varied stimulation profiles. Future development opportunities include wireless control capabilities, expanded parameter ranges, and real-time feedback mechanisms. Additionally, clinical studies could further optimize waveform patterns for specific rehabilitation protocols. This work establishes a practical foundation for advancing FES rehabilitation through more precise programmable and flexible stimulation control, potentially leading to improved rehabilitation outcomes for diverse patient populations.

ACKNOWLEDGEMENT

The authors would like to thank the Ministry of Higher Education (MOHE) Malaysia and Universiti Teknologi MARA, Cawangan Pulau Pinang, for the research facilities provided during the experimental work. The APC and research work were funded by the Ministry of Higher Education (MOHE) Malaysia through the Fundamental Research Grant Scheme (FRGS) with grant number: FRGS/1/2021/TK0/UITM/03/1.

REFERENCES

[1] S. Arof *et al.*, 'Adaptive Sliding Mode Feedback Control Algorithm for a Nonlinear Knee Extension Model', *Machines*, vol. 11, no. 7, p. 732, Jul. 2023, doi: 10.3390/machines11070732.

[2] N. Sanna, F. Ferrari, E. Ambrosini, A. L. G. Pedrocchi, and N. Tarabini, 'A sensorized FES-cycling system to quantify training performance and optimize stimulation strategies', in *2023 IEEE International Symposium on Medical Measurements and Applications (MeMeA)*, Jeju, Republic of Korea, 2023, pp. 1–5. doi: 10.1109/MeMeA57477.2023.10171920.

[3] M. K. I. Ahmad, A. Shamsudin, Z. Soomro, R. Abdul Rahim, B. Kader Ibrahim, and M. Huq, 'Closed-loop Functional Electrical Stimulation (FES) – cycling rehabilitation with phase control Fuzzy Logic for fatigue reduction control strategies for stroke patients', *SINERGI*, vol. 28, no. 1, pp. 63–74, Dec. 2023, doi: http://dx.doi.org/10.22441/sinergi.2024.1.007.

[4] M. O. Ibitoye, N. A. Hamzaid, and Y. K. Ahmed, 'Effectiveness of FES-supported leg exercise for promotion of paralysed lower limb muscle and bone health—a systematic review', *Biomed Tech (Berl)*, vol. 68, no. 4, pp. 329–350, Mar. 2023, doi: 10.1515/bmt-2021-0195.

[5] F. Naz, D. Hussain, H. Ali, Q. Raza, and F. Siddique, 'Effectiveness of functional electrical stimulation machine in managing neurological diseases - A retrospective study', *Pak J Med Sci*, vol. 40, no. 2ICON Suppl, pp. S53–S57, Jan. 2024, doi: 10.12669/pjms.40.2(ICON).8966.

[6] J. Rae-Duprees, 'A Stimulating New Direction for FES', *IEEE Pulse*, vol. 13, no. 6, pp. 12–16, Dec. 2022, doi: 10.1109/MPULS.2022.3227809.

[7] Q. Zhang, A. Iyer, K. Lambeth, K. Kim, and N. Sharma, 'Ultrasound Echogenicity as an Indicator of Muscle Fatigue during Functional Electrical Stimulation', *Sensors (Basel, Switzerland)*, vol. 22, no. 1, p. 335, 2022, doi: https://doi.org/10.3390/s22010335.

[8] A. M. Stewart, C. G. Pretty, and X. Chen, 'Design and testing of a novel, low-cost, low-voltage, functional electrical stimulator', in *2016 12th IEEE/ASME International Conference on Mechatronic and Embedded Systems and Applications (MESA)*, Auckland, New Zealand: IEEE, Aug. 2016, pp. 1–6. doi: 10.1109/MESA.2016.7587155.

[9] E. Noorsal, S. Z. Yahaya, Z. Hussain, R. Boudville, M. N. Ibrahim, and Y. Mohd Ali, 'Analytical study of flexible stimulation waveforms in muscle fatigue reduction', *IJECE*, vol. 10, no. 1, p. 690, Feb. 2020, doi: 10.11591/ijece.v10i1.pp690-703.

[10] T. Ward *et al.*, 'Multichannel Biphasic Muscle Stimulation System for Post Stroke Rehabilitation', *Electronics*, vol. 9, no. 7, p. 1156, Jul. 2020, doi: DOI: 10.3390/electronics9071156.

[11] S. Sun *et al.*, 'Function Electrical Stimulation Effect on Muscle Fatigue Based on Fatigue Characteristic Curves of Dumbbell Weightlifting Training', *Cyborg Bionic Syst.*, vol. 5, p. 0124, Jun. 2024, doi: 10.34133/cbsystems.0124.

[12] M. Sahin and Y. Tie, 'Non-rectangular waveforms for neural stimulation with practical electrodes', *J. Neural Eng.*, vol. 4, no. 3, pp. 227–233, Sep. 2007, doi: 10.1088/1741-2560/4/3/008.

[13] B. Nath *et al.*, 'A biphasic current-mode stimulator integrated circuit with a novel residual charge compensation mechanism', *Integration*, vol. 91, pp. 79–88, Jul. 2023, doi: 10.1016/j.vlsi.2023.03.003.

[14] J. A. Mercado-Gutierrez *et al.*, 'A Flexible Pulse Generator Based on a Field Programmable Gate Array Architecture for Functional Electrical Stimulation', *Front. Neurosci.*, vol. 15, p. 702781, Jan. 2022, doi: 10.3389/fnins.2021.702781.

[15] F. Saavedra, R. Osorio, P. Aqueveque, and B. Andrews, 'Effect of the Current Intensity and Inter-Electrode Distance in Surface Electrical Stimulation: A FEM Simulation Study', in *2022 44th Annual International Conference of the IEEE Engineering in Medicine & Biology Society (EMBC)*, Glasgow, Scotland, United Kingdom, 2022, pp. 752–755. doi: 10.1109/EMBC48229.2022.9871286.

[16] D. J. Kanojiya and K. Jagad, 'Functional Electrical Stimulation for Physiotherapy Management of Neurological Conditions: An Evidence Based Study', *IJSHR*, vol. 6, no. 3, pp. 422–430, 2021, doi: https://doi.org/10.52403/ijshr.20210769.

[17] W. M. Grill and J. T. Mortimer, 'Stimulus waveforms for selective neural stimulation', *IEEE Eng. Med. Biol. Mag.*, vol. 14, no. 4, pp. 375–385, Aug. 1995, doi: 10.1109/51.395310.

[18] Z.-P. Fang and J. T. Mortimer, 'Selective activation of small motor axons by quasitrapezoidal current pulses', *IEEE Trans. Biomed. Eng.*, vol. 38, no. 2, pp. 168–174, Feb. 1991, doi: 10.1109/10.76383.

[19] N. Accornero, G. Bini, G. L. Lenzi, and M. Manfredi, 'Selective Activation of peripheral nerve fibre groups of different diameter by triangular shaped stimulus pulses.', *The Journal of Physiology*, vol. 273, no. 3, pp. 539–560, Dec. 1977, doi: 10.1113/jphysiol.1977.sp012109.

[20] S. Jezernik and M. Morari, 'Energy-Optimal Electrical Excitation of Nerve Fibers', *IEEE Trans. Biomed. Eng.*, vol. 52, no. 4, pp. 740–743, Apr. 2005, doi: 10.1109/TBME.2005.844050.

[21] D. R. Cantrell and J. B. Troy, 'Extracellular stimulation of mouse retinal ganglion cells with non-rectangular voltage-controlled waveforms', in *2009 Annual International Conference of the IEEE Engineering in Medicine and Biology Society*, Minneapolis, MN: IEEE, Sep. 2009, pp. 642–645. doi: 10.1109/IEMBS.2009.5333464.

[22] Z. Z. Karu, W. K. Durfee, and A. M. Barzilai, 'Reducing muscle fatigue in FES applications by stimulating with N-let pulse trains', *IEEE Trans. Biomed. Eng.*, vol. 42, no. 8, pp. 809–817, Aug. 1995, doi: 10.1109/10.398642.

[23] P. Nadeau and M. Sawan, 'A flexible high voltage biphasic current-controlled stimulator', in *2006 IEEE Biomedical Circuits and Systems Conference*, London, UK: IEEE, Nov. 2006, pp. 206–209. doi: 10.1109/BIOCAS.2006.4600344.

[24] J. Wang, Y. Zhang, C. Liang, and Z. Tang, 'Multichannel asynchronous electrical stimulation device relieves muscle fatigue caused by stimulation therapy', in *2022 International Symposium on Control Engineering and Robotics (ISCER)*, Changsha, China: IEEE, 2022, pp. 26–30. doi: 10.1109/ISCER55570.2022.00011.

[25] Z. Hussain, H. F. Mustapha, E. Noorsal, K. A. Ahmad, and K. Sooksood, 'Flexible Biphasic Functional Electrical Stimulator for Children with Cerebral Palsy', in *2021 11th IEEE International Conference on Control System, Computing and Engineering (ICCSCE)*, Penang, Malaysia: IEEE, Aug. 2021, pp. 234–239. doi: 10.1109/ICCSCE52189.2021.9530858.

[26] V. A. Bakhtina, D. E. Goncharov, A. A. Khomchenkova, A. A. Levitskiy, P. S. Marinushkin, and N. V. Novikova, 'Encoder-Controlled Stimulation System for Assisting Elbow Extension in Post-Stroke Individuals: a Pilot Study', in *2020 International Conference on Actual Problems of Electron Devices Engineering (APEDE)*, Saratov, Russia: IEEE, Sep. 2020, pp. 279–281. doi: 10.1109/APEDE48864.2020.9255606.

[27] M. A. M. A. Halim *et al.*, 'A Low Cost and User Friendly Graphical User Interface for Programmable and Flexible FES', in *2024 IEEE 14th International Conference on Control System, Computing and Engineering (ICCSCE)*, Penang, Malaysia: IEEE, Aug. 2024, pp. 180–185. doi: 10.1109/ICCSCE61582.2024.10696463.

[28] B. Basumatary, R. S. Halder, and A. Sahani, 'A Microcontroller based Charge Balanced Trapezoidal Stimulus Generator for FES System', in *2021 IEEE International Instrumentation and Measurement Technology Conference (I2MTC)*, Glasgow, United Kingdom: IEEE, May 2021, pp. 1–4. doi: 10.1109/I2MTC50364.2021.9459837.

[29] M. G. Lakshmana Kumar, G. D. V. Santhosh Kumar, R. S. Sairam, and S. R. Krishna Vanjari, 'Flexible Functional Electrical Stimulation Architecture with External Remote Controller for Unilateral Facial Paralysis Patients', in *IECON 2018 - 44th Annual Conference of the IEEE Industrial Electronics Society*, Washington, DC: IEEE, Oct. 2018, pp. 3330–3335. doi: 10.1109/IECON.2018.8592799.

[30] M. Fenko, M. Valtin, C. Wiesener, R. Fanaei Pirlar, A. Trampuz, and T. Schauer, 'Development of a current controlled stimulation setup for investigating the effect of electrical currents on implant infections caused by biofilms', *Current Directions in Biomedical Engineering*, vol. 9, no. 1, pp. 109–112, Sep. 2023, doi: 10.1515/cdbme-2023-1028.